



**Providing Choice & Value**

Generic CT and MRI Contrast Agents

**FRESENIUS  
KABI**

**CONTACT REP**

**AJNR**

This information is current as  
of July 17, 2025.

## **Optimization of [ $^{18}\text{F}$ ]-FDOPA Brain PET Acquisition Times for Assessment of Parkinsonism in the Clinical Setting**







Graham Keir, Faizullah Mashriqi, Christopher Caravella,  
Sean A.P. Clouston, Josephine N. Rini and Ana M.  
Franceschi

*AJNR Am J Neuroradiol* 2024, 45 (6) 781-787

doi: <https://doi.org/10.3174/ajnr.A8207>

<http://www.ajnr.org/content/45/6/781>

# Optimization of [ $^{18}\text{F}$ ]-FDOPA Brain PET Acquisition Times for Assessment of Parkinsonism in the Clinical Setting

 Graham Keir,  Faizullah Mashriqi,  Christopher Caravella,  Sean A.P. Clouston,  Josephine N. Rini, and  Ana M. Franceschi



## ABSTRACT

**BACKGROUND AND PURPOSE:** Fluorine 18-fluoro-L-dopa ( $^{18}\text{F}$ -FDOPA) was approved by the FDA in 2019 and reimbursed by the Centers for Medicare & Medicaid Services in 2022 for use with PET to visualize dopaminergic nerve terminals in the striatum for evaluation of parkinsonism. We sought to determine the optimal image acquisition time for  $^{18}\text{F}$ -FDOPA PET by evaluating rater-estimated FDOPA positivity and image quality across 4 time points.

**MATERIALS AND METHODS:** Brain PET/CT was acquired 90 minutes following injection of 185 megabecquerel (5 mCi) of  $^{18}\text{F}$ -FDOPA. PET was acquired in list mode for 20 minutes, and data were replayed to represent 15-, 10-, and 5-minute acquisitions. By means of MIMneuro, PET/MR imaging or PET/CT was independently graded for FDOPA positivity and image quality by 2 readers, blinded to the clinical report and diagnosis. Expert neuroradiologist clinical reads were used as the criterion standard.

**RESULTS:** Twenty patients were included, average age 65.6 years, 55% women. Image-quality ratings decreased with shorter acquisition times for both readers (reader 1,  $\rho = 0.23$ ,  $P = .044$ ; reader 2,  $\rho = 0.24$ ,  $P = .036$ ), but there was no association between abnormality confidence scores and acquisition time (reader 1,  $\rho = -0.13$ ,  $P = .250$ ; reader 2,  $\rho = -0.19$ ,  $P = .100$ ). There was a high degree of consistency in intra- and interrater agreement and agreement with the expert reads when using acquisition times of  $\geq 10$  minutes (maximal confidence score consistency [ $\rho = 0.92$ ] and interrater agreement [ $\kappa = 0.90$ ] were observed at 15 minutes), while image quality was consistently rated as low and FDOPA positivity ratings were inconsistent when using a 5-minute acquisition time.

**CONCLUSIONS:** Our study suggests that image-quality ratings were stable after 15 minutes and that between-subject abnormality detection rates were highly consistent between the 2 readers when acquired for at least 10 and up to 20 minutes but were inconsistent at 5 minutes. Shorter  $^{18}\text{F}$ -FDOPA PET acquisition times may help maximize patient comfort while increasing throughput in the clinical setting.

**ABBREVIATIONS:** AADC = aromatic amino acid decarboxylase; AC = attenuation-corrected; DaT = dopamine transporter; PD = Parkinson disease; PS = parkinsonian syndromes

Parkinsonian syndromes (PS) are a heterogeneous group of disorders that present with motor symptoms that are mostly ascribed to idiopathic Parkinson disease (PD). This group includes PD as well as atypical PS such as multiple system atrophy,


progressive supranuclear palsy, dementia with Lewy bodies, and corticobasal degeneration. PS are distinguished from other causes of parkinsonism (essential tremor, drug-induced parkinsonism, and vascular parkinsonism) by the presence of nigrostriatal degeneration. This distinction is crucial to initiate the appropriate therapy and prevent the possible harmful effects of unsupported levodopa therapy when the symptoms mimic PD but are not neurodegenerative. Functional imaging with dopamine ligands can aid with this distinction by targeting either the presynaptic or postsynaptic dopaminergic system.<sup>1</sup>

Several radiotracers are currently used for presynaptic dopaminergic molecular imaging, with the most common being radiopharmaceuticals N-3-fluoropropyl-2-(R)-carboxymethoxy-3-(R)-(4-[iodine 123] iodophenyl) nortropane ( $^{123}\text{I}$  FP-CIT, dopamine transporter scan [DaTscan]) and 3,4-dihydroxy-6-[fluorine 18

Received November 7, 2023; accepted after revision January 25, 2024.

From the Neuroradiology Division (G.K., F.M., A.M.F.), Department of Radiology, Donald and Barbara Zucker School of Medicine at Hofstra/Northwell, Lenox Hill Hospital, New York, New York; Nuclear Medicine Division (C.C., J.N.R.), Department of Radiology, Donald and Barbara Zucker School of Medicine at Hofstra/Northwell, Manhasset, New York; and Department of Family, Population and Preventive Medicine (S.A.P.C.), Renaissance School of Medicine at Stony Brook University, Stony Brook, New York.

Please address correspondence to Ana M. Franceschi, MD, PhD, Department of Radiology, Lenox Hill Hospital, 100 East 77th St, 3rd Floor, New York, NY, 10075; e-mail: afranceschi@northwell.edu; @AFranceschi\_MDPhD

 Indicates article with online supplemental data.

<http://dx.doi.org/10.3174/ajnr.A8207>

**Table 1: [<sup>18</sup>F]-FDOPA brain PET/CT protocol<sup>a</sup>**

CT Parameters		PET Parameters	
Kilovolt (peak)	120	Acquisition (1-bed)	20-Min static acquired in list mode
Max mA (auto mA off)	95	Reconstruction	VUE Point FX <sup>b</sup>
Noise index	NA	Matrix	192 × 192
CT section thickness (mm)	3.75	Iterations	2
Rotation (sec)	0.8	Subsets	32
Pitch (mm/rot)	1.375	Z-axis filter	Heavy
FOV (cm)	50	Postfilter (mm, FWHM)	4
		FOV (cm)	30

**Note:**—Max indicates maximum; FWHM, full width at half maximum; rot, rotation; NA, not applicable; mA, milliamperé.

<sup>a</sup> Discovery 710HD scanner.

<sup>b</sup> GE Healthcare.

fluoro-L-dopa ([<sup>18</sup>F]-FDOPA).<sup>2</sup> [<sup>18</sup>F]-FDOPA is a radiolabeled analog of L-DOPA used to image metabolic abnormalities of presynaptic DaTs and L-type amino acid transporters and may be used for the assessment of PS.<sup>3</sup> Tracer accumulation in the striatum corresponds to the level of radiotracer uptake into the presynaptic nerve terminal, dopa-decarboxylase (aromatic amino acid decarboxylase [AADC]) activity, and vesicular storage in the presynaptic dopaminergic neurons.<sup>4,5</sup> Studies have demonstrated that the uptake of [<sup>18</sup>F]-FDOPA in the basal ganglia is reduced in PD,<sup>6</sup> thereby facilitating the differentiation between PS and non-neurodegenerative causes of parkinsonism. Characteristic findings in patients with PD include asymmetric reduction of [<sup>18</sup>F]-FDOPA uptake in the striatum, with greater reductions typically noted contralateral to the clinically more-affected side.<sup>7,8</sup> In addition, radiopharmaceutical binding is lowest in the posterior putamen compared with the anterior putamen and caudate nucleus, which is referred to as the rostrocaudal gradient of FDOPA uptake.<sup>9,10</sup> Reductions in [<sup>18</sup>F]-FDOPA uptake have consistently been shown to best correlate with disease severity and clinical bradykinesia scores, while the correlation with tremor, rigidity, and postural disturbance is less significant.<sup>11–15</sup>

[<sup>18</sup>F]-FDOPA has been FDA-approved to visualize dopaminergic nerve terminals in the striatum for the evaluation of adult patients with suspected PS since 2019 and received Centers for Medicare & Medicaid Services payment approval in late 2022.<sup>16,17</sup> Our current institutional protocol for [<sup>18</sup>F]-FDOPA brain PET is in accordance with the FDA prescribing guidelines<sup>18</sup> and includes list mode acquisition for 20 minutes, though acquisition times for PET vary depending on scanner sensitivity and administered dose. Notably, the highest uptake of the radiotracer in the striatum is approximately 90 minutes postinjection of [<sup>18</sup>F]-FDOPA.<sup>19,20</sup> Using dynamic acquisitions, we noted anecdotally that the clarity of the images might imply that a shorter acquisition time could be sufficient for the assessment of nigrostriatal dysfunction in the clinical setting. There are several potential benefits to a shorter acquisition time. First, patients with parkinsonism often have trouble lying still in the scanner for long periods owing to tremors or other movement disorders or cognitive impairments, so a shorter PET scan duration may improve patient comfort and reduce motion artifacts. Additionally, shorter acquisition times could allow increased throughput of patients, enabling greater access and allowing more patients the opportunity to be evaluated by this emerging technique. Therefore, we

sought to determine the optimal image acquisition time for [<sup>18</sup>F]-FDOPA brain PET by evaluating reader confidence and image quality across 4 acquisition periods.

## MATERIALS AND METHODS

We started our clinical FDOPA PET imaging service in November 2022, and the first 20 patients imaged at our institution were selected for this study. Patients were instructed to withhold PD medications, if applicable, for 12 hours before the PET scan, and followed a

low-protein diet beginning in the evening before the examination, with nothing by mouth except for water for 4 hours before the examination. All subjects were pretreated with carbidopa, 150 mg, approximately 1 hour before IV injection of 185-megabecquerel [5-mCi] [<sup>18</sup>F]-FDOPA. Brain PET/CT was acquired on a Discovery 710HD scanner (GE Healthcare) 90 minutes following injection in list mode for 20 minutes and reconstructed according to the standard institutional protocol (Table 1). Following each 20-minute acquisition, data were reconstructed to represent 15-, 10-, and 5-minute acquisition times.

Following Northwell institutional review board approval, the attenuation-corrected (AC) PET data across 4 time points were anonymized, and all indicators of acquisition time were removed, as were the CT and separately acquired brain MR imaging studies for each subject. These anonymized studies were then analyzed by 2 readers, blinded to the clinical report and final diagnosis. These 2 readers were the same for every patient and consisted of senior residents in diagnostic radiology with clinical experience reading DaTscans. Both readers participated in multiple training sessions for FDOPA PET interpretation using MIMNeuro software (Version 7.3.2; MIM Software) before study commencement. By means of MIMneuro, findings of [<sup>18</sup>F]-FDOPA PET/MR imaging or PET/CT (if MR imaging was unavailable) were independently graded for reader confidence on the likely FDOPA positivity of an image using a 5-point scale (0 = definitely normal, 1 = probably normal, 2 = equivocal, 3 = probably abnormal, 4 = definitely abnormal). For analyses of inter- and intrarater agreement and when comparing scores with the expert rater, confidence scores were dichotomized to indicate the presence/absence of abnormal findings using a cutoff of ≥3 (probably abnormal). Image quality was graded on a 3-point scale (1 = poor quality, 2 = acceptable, 3 = excellent); poor-quality images were those rated as 1 in this scale.

Expert clinical reads by a board-certified fellowship-trained neuroradiologist with an MD/PhD and 10 years of brain PET/MR imaging clinical and research experience were used as the criterion standard.

## Statistical Analysis

Sample characteristics were described using means (SDs) or percentages if appropriate and stratified by neuroradiology expert reads (Tables 2 and 3). Nonparametric trend tests were used to determine whether demographic characteristics, image quality,

and abnormality confidence scores varied by FDOPA abnormality. Next, intraindividual consistency was measured using the Spearman rank-order correlation within individuals to determine the extent to which FDOPA images were rated consistently in terms of confidence of abnormal findings and image quality across scanning parameters. Because the Spearman  $\rho$  may be biased in cases in which rankings remain stable though average scores differ, the Cohen  $\kappa$  was also used to examine the presence/absence of

abnormal imaging findings for all rater times and when comparing raters and the neuroradiologist's expert reads. To visually differentiate these measures, we used a different cell color (red, green, and blue) to differentiate the test type; then darker hues of each color were used to indicate stronger associations (Table 4). Two-tailed  $t$  tests were used to examine the statistical significance of the Spearman  $\rho$  and Cohen  $\kappa$  in all tests. Because of the large number of comparisons and the small sample size made

up of relatively unique patients, statistical significance in the final analyses was reported in 2 ways. Bold italicized typeface was used to report statistically significant results that passed the false discovery rate (0.05). Supplemental analyses were completed to examine image-quality ratings using  $\chi^2$  tests to estimate the impact of acquisition time on the raters' ratings of image quality. However, while we did attempt to account for image-quality rankings when considering positivity scores, due to the small sample size, these efforts were unsuccessful in most cases and these analyses are not presented. Analyses were completed by using STATA 17/MP (StataCorp).

## RESULTS

Demographic and clinical characteristics for  $n = 20$  subjects included in the study are depicted in Tables 2 and 3. The patients had an average age of 65.6 years, and 55% were women. No differences were evident in demographic characteristics between groups, but the confidence and quality scores differed between groups across all ratings. In general, the scans rated by the neuroradiologist's expert read as having abnormal findings had higher confidence scores and lower image-quality ratings than those rated as having normal findings.

Per the neuroradiologist's expert read, 10 studies (50%) had abnormal findings as evaluated at the standard 20-minute acquisition time (Fig 1). There was no association between reader confidence and acquisition time (reader 1,  $\rho = -0.13$ ,  $P = .250$ ; reader 2,  $\rho = -0.19$ ,  $P = .100$ ). However, image-quality ratings were lower among images with shorter acquisition times for both reviewers (reader 1,  $\rho = 0.23$ ,  $P = .044$ ; reader 2,  $\rho = 0.24$ ,  $P = .036$ ) (Figs 2 and 3).

**Table 2: Demographic characteristics for subjects ( $n = 20$ ) stratified by neuroradiologist expert read results at the standard 20-minute acquisition time**

Characteristic	Whole Sample ( $n = 20$ )	Expert Rated Scan Findings as Abnormal ( $n = 10$ )	Expert Rated Scan Findings as Normal ( $n = 10$ )	P Value
Age (yr)	65.6 (14.9)	62.8 (17.4)	68.4 (12.3)	.402
Female (%)	55.0	40.0	70.0	.189
Clinical history				
Tremor in hand/leg (%)	60.0	70.0	50.0	.361
PD (%)	15.0	30.0	0.0	.060
Right unilateral (%)	10.0	10.0	10.0	1.000
Left unilateral (%)	20.0	30.0	10.0	.264
Bilateral (%)	20.0	20.0	20.0	1.000
Bradykinesia (%)	25.0	50.0	0.0	.010

**Table 3: Reader confidence and image quality scores stratified by neuroradiologist expert read results at the standard 20-minute acquisition time<sup>a</sup>**

	Whole Sample ( $n = 20$ )	Expert Rated Scan Findings as Abnormal ( $n = 10$ )	Expert Rated as Scan Findings as Normal ( $n = 10$ )	P Value
Confidence score (mins)				
20	1.6 (1.4)	2.9 (0.8)	0.4 (0.5)	<.001
15	1.8 (1.4)	3 (0.7)	0.6 (0.5)	<.001
10	2 (1.5)	3.3 (0.7)	0.7 (0.9)	<.001
5	2.2 (1.3)	3 (0.9)	1.4 (1)	.001
Image quality (mins)				
20	2.2 (0.7)	1.8 (0.7)	2.6 (0.6)	.003
15	2.2 (0.8)	1.8 (0.7)	2.6 (0.6)	.004
10	2 (0.9)	1.6 (0.7)	2.5 (0.8)	.006
5	1.7 (0.8)	1.3 (0.5)	2.2 (0.9)	.009

<sup>a</sup>No differences between scans with abnormal and normal findings were statistically significant as determined using nonparametric trend tests.

**Table 4: Measures of image-rating agreement and consistency across the 2 raters and the expert neuroradiologist read using different acquisition times<sup>a</sup>**

Rater	Minutes	First Rater				Second Rater			
		20	15	10	5	20	15	10	5
First rater	20	<b>0.70</b>	<b>0.79</b>	<b>0.89</b>	<b>0.79</b>	<b>0.56</b>	<b>0.89</b>	<b>0.61</b>	0.22
	15	<b>0.89</b>	<b>0.90</b>	<b>0.90</b>	<b>1.00</b>	<b>0.79</b>	<b>0.90</b>	<b>0.80</b>	0.41
	10	<b>0.93</b>	<b>0.93</b>	<b>0.80</b>	<b>0.90</b>	<b>0.68</b>	<b>0.79</b>	<b>0.71</b>	0.31
	5	<b>0.84</b>	<b>0.85</b>	<b>0.84</b>	<b>0.90</b>	<b>0.79</b>	<b>0.90</b>	<b>0.80</b>	0.41
Second rater	20	<b>0.84</b>	<b>0.80</b>	<b>0.83</b>	<b>0.88</b>	<b>0.70</b>	<b>0.68</b>	<b>0.61</b>	0.22
	15	<b>0.87</b>	<b>0.92</b>	<b>0.87</b>	<b>0.83</b>	<b>0.84</b>	<b>0.80</b>	<b>0.71</b>	0.31
	10	<b>0.81</b>	<b>0.87</b>	<b>0.83</b>	<b>0.77</b>	<b>0.82</b>	<b>0.83</b>	<b>0.90</b>	0.39
	5	<b>0.55</b>	<b>0.44</b>	<b>0.55</b>	<b>0.53</b>	<b>0.54</b>	<b>0.45</b>	<b>0.64</b>	<b>0.50</b>

<sup>a</sup>Rank order agreement is shown in blue; intra-/interrater agreement across image ratings is shown in green. The correspondence of confidence scores to the expert neuroradiologist read completed at a standard 20-minute acquisition time is shown in shades of red across the diagonal. The strength of the association is reported by color gradations. Statistically significant associations evident after adjusting for the false discovery rate are shown in bold italicized typeface. The optimal cutoff for rater 1 compared with the expert rating included scans rated as equivocal, while the optimal cutoff for rater 2 compared with expert raters included only those with a probable abnormal finding and above.



Analysis of interrater reliability (Table 4) revealed that an abnormal finding on an image was rated similarly between readers at 20-, 15-, and 10-minute acquisition times. However, the interrater confidence scores were inconsistent across raters and between

the raters and the expert neuroradiologist read at 5 minutes. In contrast, ratings were relatively consistent both in terms of rank order and abnormality agreement when using image-acquisition times of 10–15 minutes. Of interest, the maximal

association in confidence scores between raters occurred at 15 minutes ( $\rho = 0.92$ ), while the maximal  $\kappa$  when comparing raters also occurred at 15 minutes ( $\kappa = 0.90$ ).

Not shown as main results are examinations of image-quality ratings made by the 2 readers (Online Supplemental Data), which showed relatively less consistent results. For example, the raters consistently scored image quality lower when acquisition times were 5 minutes ( $\rho = 0.68$ ,  $P = .001$ ), compared with 10-minute ( $\rho = 0.36$ ,  $P = .124$ ), 15-minute ( $\rho = 0.43$ ,  $P = .058$ ), or 20-minute ( $\rho = 0.29$ ,  $P = .209$ ) acquisition times. Raters agreed that image quality was poor in most scans when using a 5-minute acquisition time (Online Supplemental Data).

## DISCUSSION

Functional imaging with dopamine ligands targets the dopaminergic system and is currently used to aid with the distinction of PD from other conditions that mimic the disease. Following the FDA approval of [ $^{18}\text{F}$ ]-FDOPA PET in 2019, which was obtained on the basis of a clinical trial of 56 patients with suspected PS,<sup>16,21</sup> we introduced [ $^{18}\text{F}$ ]-FDOPA PET into practice and incorporated this study into our routine clinical

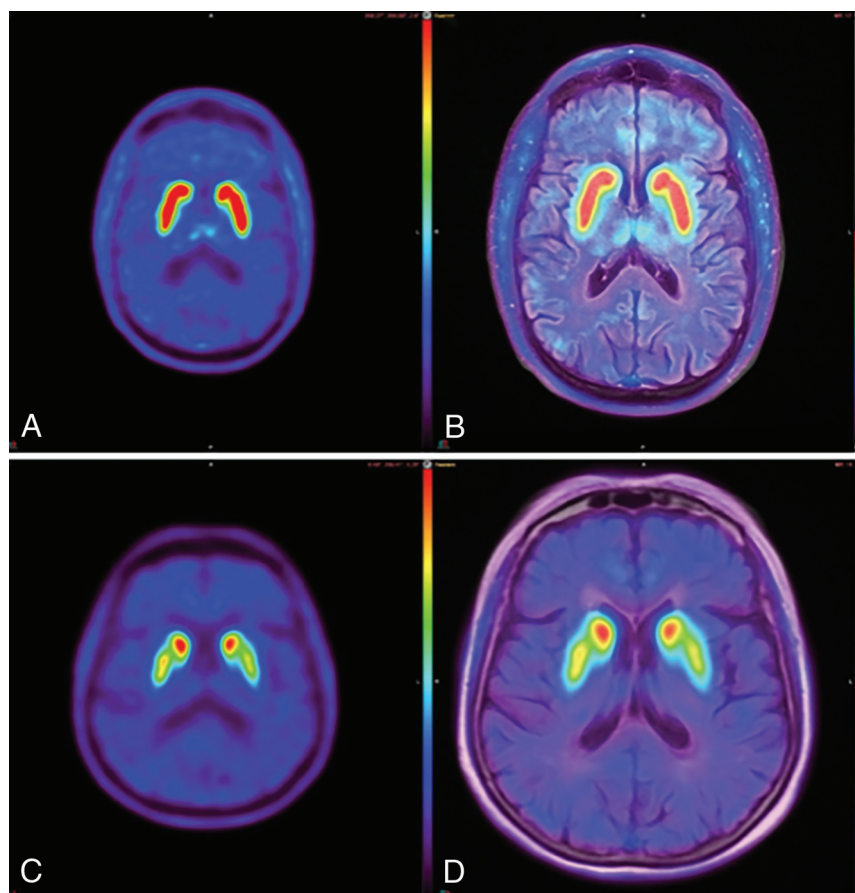


**FIG 1.** [ $^{18}\text{F}$ ]-FDOPA brain PET and fused [ $^{18}\text{F}$ ]-FDOPA brain PET/MR imaging at a standard 20-minute acquisition time. The healthy subject (A and B) demonstrates the characteristic “comma sign” uptake in the striatum. The subject with abnormal findings (C and D) demonstrates marked loss of uptake in the bilateral striatum, particularly involving the bilateral putamina and left > right caudate nuclei, corresponding to more extensive right-sided clinical deficits.

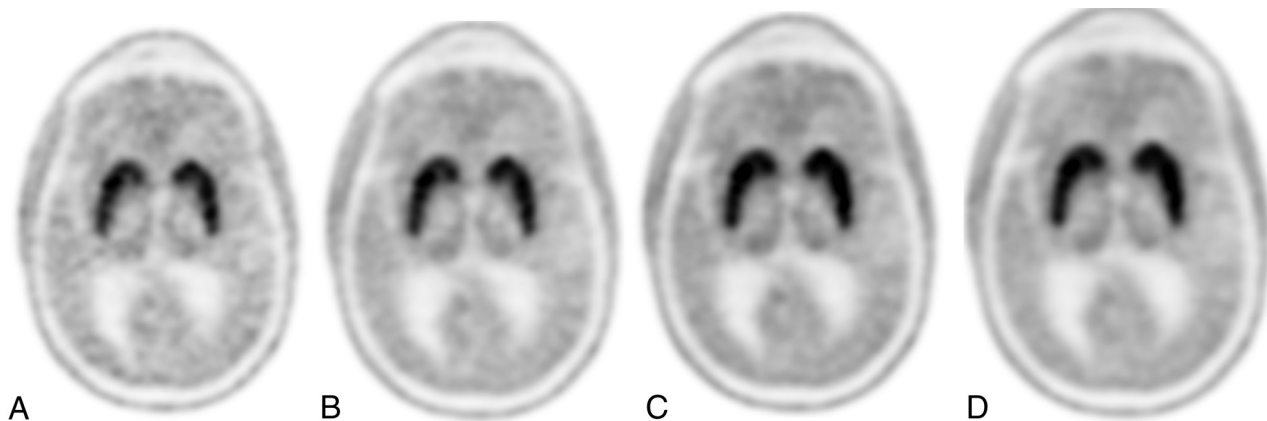


**FIG 2.** Normal findings on [ $^{18}\text{F}$ ]-FDOPA AC PET at 5-minute (A), 10-minute (B), 15-minute (C), and 20-minute (D) acquisition times. Note that image-quality ratings were stable following 15 minutes, and between-subject abnormality detection rates were highly consistent between the 2 readers when using 10-, 15-, or 20-minute acquisition times but were inconsistent at 5 minutes.

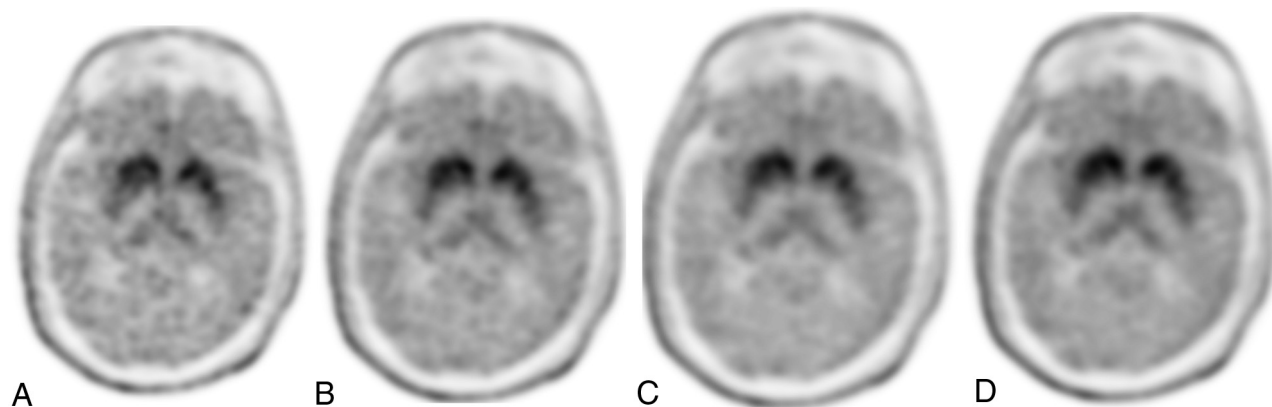


**FIG 3.** Abnormal findings on [ $^{18}\text{F}$ ]-FDOPA AC PET at 5-minute (A), 10-minute (B), 15-minute (C), and 20-minute (D) acquisition times. Note that image-quality ratings were stable following 15 minutes, and between-subject abnormality detection rates were highly consistent between the 2 readers when using 10-, 15-, or 20-minute acquisition times but were inconsistent at 5 minutes.

workflow for PD assessment, because it is currently reimbursed by the Centers for Medicare & Medicaid Services in the United States.<sup>17</sup> The present study sought to examine the influence of imaging-parameter selection and quality on abnormality ratings and found that the optimal acquisition times for [ $^{18}\text{F}$ ]-FDOPA PET for clinical purposes was approximately 10–15 minutes.

The European Association of Nuclear Medicine and the Society of Nuclear Medicine and Molecular Imaging have developed joint clinical practice guidelines that address clinical and technical aspects of dopaminergic imaging for patients with PS, to assist radiologists in recommending, performing, interpreting, and reporting the results of dopaminergic imaging in patients with PS.<sup>22</sup> Per these guidelines, the diagnostic importance of presynaptic dopaminergic imaging (ie, [ $^{18}\text{F}$ ]-FDOPA PET; DaT SPECT) is the following: 1) to support the differential diagnosis between essential tremor and neurodegenerative PS;<sup>23–26</sup> 2) to help distinguish dementia with Lewy bodies and other dementias (in particular, Alzheimer disease);<sup>27–29</sup> 3) to support the differential diagnosis between PS due to presynaptic degenerative dopamine deficiency and other forms of PS (eg, drug-induced, psychogenic, or vascular parkinsonism);<sup>30–32</sup> and 4) to detect early presynaptic PS.<sup>33,34</sup>

The goal of [ $^{18}\text{F}$ ]-FDOPA PET visual assessment is to qualitatively analyze uptake in the striatum (putamen and caudate nucleus) by setting the maximum color scale value to the maximal tracer value in the striatum. Moreover, [ $^{18}\text{F}$ ]-FDOPA not only allows qualitative interpretation, but there are established quantitative parameters that can be calculated to objectively quantify the degree of striatal neuronal loss.<sup>35–38</sup> Semiquantitative analysis may be performed in the clinical setting, typically by calculating the striato-occipital ratio, which has been shown to correlate with clinical disability ratings.<sup>35</sup> Quantitative analysis of dynamic time-activity curves may also be used to determine multiple aspects of [ $^{18}\text{F}$ ]-FDOPA influx constants (Ki maps).<sup>36</sup> For example, Dhawan et al<sup>38</sup> demonstrated a graphic approach to compare the striatal-to-occipital ratio and influx constant in [ $^{18}\text{F}$ ]-FDOPA PET studies, highlighting a similar accuracy using a short 10-minute scan at 95 minutes post-radiopharmaceutical injection. Similarly, in our study, visual image-quality ratings were stable following 15 minutes, and between-subject abnormality detection

rates were highly consistent between 2 readers when using 10-, 15-, or 20-minute acquisition times but were inconsistent at 5 minutes. While acquisition times for PET vary depending on the scanner sensitivity and the administered dose, these results suggest that neuroradiologists may consistently and reliably interpret [ $^{18}\text{F}$ ]-FDOPA PET at acquisition times shorter than the traditionally used 20 minutes.

Several studies have found that [ $^{18}\text{F}$ ]-FDOPA PET and the DaTscan are highly accurate and diagnose PD with similar levels of sensitivity and specificity.<sup>2,19,39</sup> There are several major advantages that favor the use of [ $^{18}\text{F}$ ]-FDOPA PET over DaT SPECT.<sup>2,39–42</sup> These include improved image resolution ( $\sim 5\text{mm}$  for PET versus  $\sim 13\text{--}14\text{ mm}$  for SPECT), shorter imaging sessions, lower radiation burden, similar-to-reduced cost, and no risk of potential iodine-induced thyroid-related side effects and therefore no need for the administration of the Lugol solution before the examination to fully saturate the thyroid to protect it from radiation exposure.<sup>41</sup> Furthermore, the ability to fuse [ $^{18}\text{F}$ ]-FDOPA PET with either CT or MR structural imaging and the introduction of simultaneous PET/MR imaging scanners for the assessment of movement disorders provides the ability to correlate with concurrent anatomic abnormalities (eg, lacunar infarcts in the striatum; enlarged perivascular spaces), which may provide added value and help confirm or exclude the existence of concomitant pathologies.<sup>43</sup>

There are several limitations to [ $^{18}\text{F}$ ]-FDOPA PET dopaminergic imaging. For example, Wallert et al<sup>40</sup> suggested that [ $^{18}\text{F}$ ]-FDOPA PET may be less sensitive than DaTscans in patients with clinically uncertain PS in the clinical setting. This suggestion may relate to the challenges of interpretation in routine practice outside the research setting. A meta-analysis has also suggested that the decrease in activity in the striatum of patients with PD is consistently smaller in studies assessing [ $^{18}\text{F}$ ]-FDOPA PET compared with DaT SPECT.<sup>10</sup> Furthermore, in early disease, there is a relative increase in [ $^{18}\text{F}$ ]-FDOPA uptake compared with vesicle monoamine transporter 2 imaging, with the radiotracer carbon 11 [ $^{11}\text{C}$ ] dihydrotetrabenazine likely corresponding to compensatory upregulation of AADC activity in early-stage PD.<sup>5</sup> Finally, limitations specific to our study include its relatively small sample size, lack of quantitative analyses (we focused on visual interpretation

only in an attempt to closely mimic routine clinical practice), and absence of long-term follow-up of study subjects for clinical monitoring of disease progression.

## CONCLUSIONS

[<sup>18</sup>F]-FDOPA PET is a promising emerging technique for the assessment of parkinsonism. Despite several minor limitations, our study suggests that image-quality ratings were stable at 10–15 minutes, and that between-subject abnormality detection rates were highly consistent between 2 readers when using 10-, 15-, or 20-minute acquisition times but were inconsistent at 5 minutes. As this novel dopaminergic imaging technique translates into clinical practice, shorter PET acquisition times may help maximize patient comfort while increasing throughput in the clinical setting.

**Disclosure forms** provided by the authors are available with the full text and PDF of this article at [www.ajnr.org](http://www.ajnr.org).

## REFERENCES

1. Ponisio MR, Iranpour P, Benzinger T. **FDOPA in Movement Disorders and Neuro-Oncology.** In: Franceschi AM, Franceschi D. eds. *Hybrid PET/MR Neuroimaging: A Comprehensive Approach.* Springer-Verlag; 2022:121–35
2. Eshuis SA, Jager PL, Maguire RP, et al. **Direct comparison of FP-CIT SPECT and F-DOPA PET in patients with Parkinson's disease and healthy controls.** *Eur J Nucl Med Mol Imaging* 2009;36:454–62 [CrossRef Medline](#)
3. Chondrogiannis S, Marzola MC, Al-Nahhas A, et al. **Normal biodistribution pattern and physiologic variants of 18F-DOPA PET imaging.** *Nucl Med Commun* 2013;34:1141–49 [CrossRef Medline](#)
4. Buu NT. **Vesicular accumulation of dopamine following L-DOPA administration.** *Biochem Pharmacol* 1989;38:1787–92 [CrossRef Medline](#)
5. Lee CS, Samii A, Sossi V, et al. **In vivo positron emission tomographic evidence for compensatory changes in presynaptic dopaminergic nerve terminals in Parkinson's disease.** *Ann Neurol* 2000;47:493–503 [CrossRef Medline](#)
6. Morrish PK, Sawle GV, Brooks DJ. **An [18F]dopa-PET and clinical study of the rate of progression in Parkinson's disease.** *Brain* 1996;119(Pt 2):585–91 [CrossRef Medline](#)
7. Leenders KL, Salmon EP, Tyrrell P, et al. **The nigrostriatal dopaminergic system assessed in vivo by positron emission tomography in healthy volunteer subjects and patients with Parkinson's disease.** *Arch Neurol* 1990;47:1290–98 [CrossRef Medline](#)
8. Bruck A, Aalto S, Rauhala E, et al. **A follow-up study on 6-[18F]fluoro-L-dopa uptake in early Parkinson's disease shows nonlinear progression in the putamen.** *Mov Disord* 2009;24:1009–15 [CrossRef Medline](#)
9. Calabria FF, Calabria E, Gangemi V, et al. **Current status and future challenges of brain imaging with (18)F-DOPA PET for movement disorders.** *Hell J Nucl Med* 2016;19:33–41 [CrossRef Medline](#)
10. Kaasinen V, Vahlberg T. **Striatal dopamine in Parkinson disease: a meta-analysis of imaging studies.** *Ann Neurol* 2017;82:873–82 [CrossRef Medline](#)
11. Ghaemi M, Raethjen J, Hilker R, et al. **Monosymptomatic resting tremor and Parkinson's disease: a multitracer positron emission tomographic study.** *Mov Disord* 2002;17:782–88 [CrossRef Medline](#)
12. Broussolle E, Dentesangle C, Landais P, et al. **The relation of putamen and caudate nucleus 18F-Dopa uptake to motor and cognitive performances in Parkinson's disease.** *J Neurol Sci* 1999;166:141–51 [CrossRef Medline](#)
13. Eidelberg D, Moeller JR, Dhawan V, et al. **The metabolic anatomy of Parkinson's disease: complementary [18F]fluorodeoxyglucose and [18F]fluorodopa positron emission tomographic studies.** *Mov Disord* 1990;5:203–13 [CrossRef Medline](#)
14. Vingerhoets FJ, Schulzer M, Calne DB, et al. **Which clinical sign of Parkinson's disease best reflects the nigrostriatal lesion?** *Ann Neurol* 1997;41:58–64 [CrossRef Medline](#)
15. Otsuka M, Ichiya Y, Kuwabara Y, et al. **Differences in the reduced 18F-Dopa uptakes of the caudate and the putamen in Parkinson's disease: correlations with the three main symptoms.** *J Neurol Sci* 1996;136:169–73 [CrossRef Medline](#)
16. Food and Drug Administration. **Drug Trials Snapshots: Fluorodopa F 18.** <https://www.fda.gov/drugs/drug-trials-snapshots-fluorodopa-f-18>. Accessed: July 7, 2023
17. Centers for Medicare and Medicaid Services. **Billing and Coding: Positron Emission Tomography Scans Coverage.** <https://www.cms.gov/medicare-coverage-database/view/article.aspx?articleid=54666>. Accessed July 7, 2023
18. Food and Drug Administration. **Highlights of Prescribing Information.** October 22, 2019. [https://www.accessdata.fda.gov/drugsatfda\\_docs/label/2019/200655s000lbl.pdf](https://www.accessdata.fda.gov/drugsatfda_docs/label/2019/200655s000lbl.pdf). Accessed: July 7, 2023
19. Ishikawa T, Dhawan V, Kazumata K, et al. **Comparative nigrostriatal dopaminergic imaging with iodine-123-beta CIT-FP/SPECT and fluorine-18-FDOPA/PET.** *J Nucl Med* 1996;37:1760–65 [Medline](#)
20. Dhawan V, Ishikawa T, Patlak C, et al. **Combined FDOPA and 3OMFD PET studies in Parkinson's disease.** *J Nucl Med* 1996;37:209–16 [Medline](#)
21. Food and Drug Administration. <https://www.fda.gov/drugs/drug-approvals-and-databases/drug-trials-snapshots-fluorodopa-f-18>. Accessed: March 21, 2024
22. Morbelli S, Esposito G, Arbizu J, et al. **EANM practice guideline/SNMMI procedure standard for dopaminergic imaging in Parkinsonian syndromes 1.0.** *Eur J Nucl Med Mol Imaging* 2020;47:1885–912 [CrossRef Medline](#)
23. Benamer TS, Patterson J, Grosset DG, et al. **Accurate differentiation of parkinsonism and essential tremor using visual assessment of [123I]-FP-CIT SPECT imaging: the [123I]-FP-CIT study group.** *Mov Disord* 2000;15:503–10 [CrossRef](#)
24. Booi J, Hemelaar TG, Speelman JD, et al. **One-day protocol for imaging of the nigrostriatal dopaminergic pathway in Parkinson's disease by [123I]FPCIT SPECT.** *J Nucl Med* 1999;40:753–61 [Medline](#)
25. Scherfler C, Schwarz J, Antonini A, et al. **Role of DAT-SPECT in the diagnostic work up of parkinsonism.** *Mov Disord* 2007;22:1229–38 [CrossRef Medline](#)
26. Nicastrò N, Garibotto V, Burkhard PR. **123I-FP-CIT SPECT accurately distinguishes parkinsonian from cerebellar variant of multiple system atrophy.** *Clin Nucl Med* 2018;43:e33–36 [CrossRef Medline](#)
27. McKeith I, O'Brien J, Walker Z, et al; DLB Study Group. **Sensitivity and specificity of dopamine transporter imaging with 123I-FP-CIT SPECT in dementia with Lewy bodies: a Phase III, multicentre study.** *Lancet Neurol* 2007;6:305–13 [CrossRef Medline](#)
28. Thomas AJ, Attems J, Colloby SJ, et al. **Autopsy validation of 123I-FP-CIT dopaminergic neuroimaging for the diagnosis of DLB.** *Neurology* 2017;88:276–83 [CrossRef Medline](#)
29. McKeith IG, Boeve BF, Dickson DW, et al. **Diagnosis and management of dementia with Lewy bodies: fourth consensus report of the DLB Consortium.** *Neurology* 2017;89:88–100 [CrossRef Medline](#)
30. Lorberboym M, Treves TA, Melamed E, et al. **[123I]-FP/CIT SPECT imaging for distinguishing drug-induced parkinsonism from Parkinson's disease.** *Mov Disord* 2006;21:510–14 [CrossRef Medline](#)
31. Felicio AC, Godeiro-Junior C, Moriyama TS, et al. **Degenerative parkinsonism in patients with psychogenic parkinsonism: a dopamine transporter imaging study.** *Clin Neurol Neurosurg* 2010;112:282–85 [CrossRef Medline](#)
32. Brigo F, Matinella A, Erro R, et al. **[123I]FP-CIT SPECT (DaTSCAN) may be a useful tool to differentiate between Parkinson's disease and vascular or drug-induced parkinsonisms: a meta-analysis.** *Eur J Neurol* 2014;21:1369–90 [CrossRef Medline](#)
33. Bauckneht M, Chincarini A, De Carli F, et al. **Presynaptic dopaminergic neuroimaging in REM sleep behavior disorder: a systematic review and meta-analysis.** *Sleep Med Rev* 2018;41:266–74 [CrossRef Medline](#)

34. Berg D, Postuma RB, Adler CH, et al. **MDS research criteria for prodromal Parkinson's disease.** *Mov Disord* 2015;30:1600–11 [CrossRef](#) [Medline](#)
35. Takikawa S, Dhawan V, Chaly T, et al. **Input functions for 6-[fluorine-18]fluorodopa quantitation in parkinsonism: comparative studies and clinical correlations.** *J Nucl Med* 1994;35:955–63 [Medline](#)
36. Sossi VD, La Fuente-Fernandez R, Holden JE, et al. **Increase in dopamine turnover occurs early in Parkinson's disease: evidence from a new modeling approach to PET 18 F-fluorodopa data.** *J Cereb Blood Flow Metab* 2002;22:232–39 [CrossRef](#) [Medline](#)
37. Hazut Krauthammer S, Cohen D, Even-Sapir E, et al. **Beyond visual assessment of basal ganglia uptake: can automated method and pineal body uptake assessment improve identification of nigrostriatal dysfunction on 18F-DOPA PET/CT?** *Int J Mol Sci* 2023;24:5683 [CrossRef](#) [Medline](#)
38. Dhawan V, Ma Y, Pillai V, et al. **Comparative analysis of striatal FDOPA uptake in Parkinson's disease: ratio method versus graphical approach.** *J Nucl Med* 2002;43:1324–30 [Medline](#)
39. Huang WS, Chiang YH, Lin JC, et al. **Crossover study of (99m)Tc-TRODAT-1 SPECT and (18)F-FDOPA PET in Parkinson's disease patients.** *J Nucl Med* 2003;44:999–1005 [Medline](#)
40. Wallert E, Letort E, van der Zant F, et al. **Comparison of [18F]-FDOPA PET and [123I]-FP-CIT SPECT acquired in clinical practice for assessing nigrostriatal degeneration in patients with a clinically uncertain parkinsonian syndrome.** *EJNMMI Res* 2022;12:68 [CrossRef](#) [Medline](#)
41. Dhawan V, Niethammer MH, Lesser ML, et al. **Prospective F-18 FDOPA PET imaging study in human PD.** *Nucl Med Mol Imaging* 2022;56:147–57 [CrossRef](#) [Medline](#)
42. Khamis K, Giladi N, Levine C, et al. **The added value of 18F-FDOPA PET/CT in the work-up of patients with movement disorders.** *Neurographics* 2019;9:344–48 [CrossRef](#)
43. Struck AF, Hall LT, Kusmirek JE, et al. **(18)F-DOPA PET with and without MRI fusion, a receiver operator characteristics comparison.** *Am J Nucl Med Mol Imaging* 2012;2:475–82 [Medline](#)